

Myocardial Kinematics From Tagged MRI Based on a 4-D B-Spline Model

Nicholas J. Tustison, Victor G. Dávila-Román, and Amir A. Amini*

Abstract—Current research investigating the modeling of left ventricular dynamics for accurate clinical assessment of cardiac function is extensive. Magnetic resonance (MR) tagging is a functional imaging method which allows for encoding of a grid of signal voids on cardiac MR images, providing a mechanism for noninvasive measurement of intramural tissue deformations, *in vivo*. We present a novel technique of employing a four-dimensional (4-D) B-spline model which permits concurrent determination of myocardial beads and myocardial strains. The method entails fitting the knot planes of the 4-D B-spline model for fixed times to a sequence of triplets of orthogonal sets of tag surfaces for all imaged volumetric frames within the constraints of the model's spatio-temporal internal energy. From a three-dimensional (3-D) displacement field, the corresponding long and short-axis Lagrangian normal, shear, and principal strain maps are produced. As an important byproduct, the points defined by the 3-D intersections of the triplets of orthogonal tag planes, which we refer to as myocardial beads, can easily be determined by our model. Displaying the beads as a movie loop allows for the visualization of the nonrigid movement of the left ventricle in 3-D.

Index Terms—B-splines, cardiac motion, myocardial beads, myocardial strain, tagged MRI.

I. INTRODUCTION

Noninvasive imaging techniques for assessing the dynamic behavior of the human heart, such as magnetic resonance (MR) tagging, are invaluable in the diagnosis of myocardial diseases. MR tagging methods allow for noninvasive measurement of intramural heart wall motion by combining the high spatio-temporal resolution of MR imaging (MRI) with tissue tagging techniques [1]. The advantages of tagged MRI have encouraged significant research in this area [2]–[8]. This paper makes the following contributions.

- Components of the model have been modified in order to enhance the model's ability to better fit the tag lines: these include use of an internal energy function, and use of additional control points for more localized interpolation of *in vivo* data.
- Myocardial strains may easily be derived from the model. Results from human data are provided in this paper.
- Tag surface intersections, referred to as myocardial beads, are easily reconstructed using the model. Results from human data are provided in this paper.

II. 4-D B-SPLINE MODEL

The four-dimensional (4-D) B-spline model [three-dimensional (3-D) B-solid + one-dimensional B-spline interpolation over time] is specified by a 4-D grid of control points to interpolate tag information across space and across all continuous time points. Data from each time frame are represented by a 3-D B-spline model specified at an

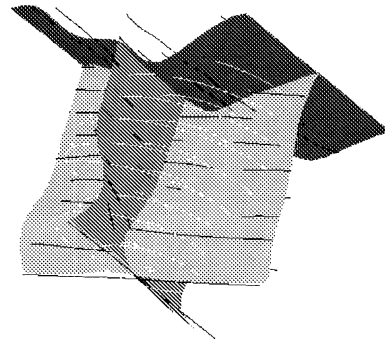


Fig. 1. Three intersecting isoparametric planes of the 4-D B-spline model at a specific time instant for an *in vivo* human data set. These isoparametric planes interpolate the tag lines in the three orthogonal directions for each time frame. The interpolated tag lines are drawn on the isoparametric planes. The endocardial and epicardial contours are also visible.

integer parametric time value (knot solid). Similarly, tag planes in each of the three orthogonal directions are specified by knot planes of the corresponding B-solid. These knot planes are isoparametric planes of the B-solid at integer parametric values. The 4-D B-spline model can be expressed as the tensor product

$$\mathbf{S}(u, v, w, t) = \sum_{i=1}^I \sum_{j=1}^J \sum_{k=1}^K \sum_{l=1}^L \mathbf{p}_{ijkl} N_{i,d}(u) N_{j,e}(v) N_{k,f}(w) N_{l,g}(t) \quad (1)$$

where $(I \times J \times K \times L)$ is the total number of control points specified by \mathbf{p}_{ijkl} and $d, e, f,$ and g designate the order of B-spline. The respective periodic B-spline basis functions which weight the contribution of the control points to the model are $N_{i,d}(u), N_{j,e}(v), N_{k,f}(w),$ and $N_{l,g}(t)$.

The fitting process is specified in a computational framework by optimizing an objective function which encodes the distance between model isoparametric planes and MRI tag planes. This optimization problem is numerically solved by the preconditioned conjugate gradient descent algorithm [10] which seeks to minimize the linear combination of the model's external and internal energies. Once the fitting process is complete, we have a time-varying B-spline solid whose isoparametric planes reconstruct the tag surfaces in the three orthogonal directions (an orthogonal grid of tag planes intersecting a stack of short-axis image slices, and a sequence of parallel tag planes intersecting long-axis images) for all continuous time points. Fig. 1 shows three orthogonal isoparametric planes of the 4-D B-spline model after fitting at a specific time instant. As can be seen, the isoparametric planes of the model interpolate their corresponding sets of tag lines in 3-D space.

III. KINEMATIC VARIABLES

At the conclusion of fitting the 4-D B-spline model to a short-axis and long-axis dynamic tagged image volume, 3-D motion and strain fields as well as 3-D tag intersections are immediately available for all continuous time points in the cardiac cycle.

A. Three-Dimensional Motion Field

The 4-D B-spline model can be used to directly extract 3-D myocardial displacement fields. By subtracting the 3-D B-solid specified at the initial time frame $t = \tau_o$ from the 3-D B-solid specified at $t = \tau$

Manuscript received August 26, 2002; revised February 8, 2003. This work was supported in part by the National Institutes of Health (NIH) under Grant HL-57628, Grant HL-58878, and Grant HL-64217. Asterisk indicates corresponding author.

N. J. Tustison and V. G. Dávila-Román are with the Cardiovascular Image Analysis Laboratory, Washington University, St. Louis, MO 63110 USA.

*A. A. Amini is with the Cardiovascular Image Analysis Laboratory, Washington University, Box 8086, 660 S. Euclid Ave., St. Louis, MO 63110 USA (e-mail: amini@cauchy.wustl.edu; website: <http://www-cv.wustl.edu>)

Digital Object Identifier 10.1109/TBME.2003.814530

[see (2)], we can describe the motion of material points within the myocardium between the two time points.

$$V(u, v, w) = \langle \mu, \nu, \xi \rangle = \mathbf{S}(u, v, w, \tau) - \mathbf{S}(u, v, w, \tau_o). \quad (2)$$

Time τ_o is the reference undeformed state which usually corresponds to end-diastole when the tags are undeformed.

B. Strain

Strain is a dimensionless quantity measuring the percent change in length at different points of a deforming continuous body. Once a displacement vector field is available, the strain of deformation can be computed at all myocardial points.

Lagrangian strain [9] maps are produced by describing the deformation of the left ventricle in the Lagrangian reference frame. If the spatial coordinates are represented by \mathbf{X} at time τ_o and by \mathbf{x} at time τ then, in the Lagrangian reference frame, the mapping $\Gamma(\mathbf{X})$ warps \mathbf{X} into \mathbf{x} ; that is $\mathbf{x} = \Gamma(\mathbf{X}) = \mathbf{V}(\mathbf{X}) + \mathbf{X}$. The deformation gradient tensor can be written as $\mathbf{F} = \nabla \Gamma(\mathbf{X}) = \nabla \mathbf{V}(\mathbf{X}) + \mathbf{I}$. The Lagrangian strain tensor \mathbf{E} is then given by

$$\mathbf{E} = \frac{1}{2} (\mathbf{F}^T \mathbf{F} - \mathbf{I}) \quad (3)$$

where \mathbf{I} is the identity matrix. The quantity $\mathbf{M}^T \mathbf{E} \mathbf{M}$ will give the value of the normal strain in the direction given by the unit vector \mathbf{M} . Due to the ventricular geometry, it is appropriate to calculate the myocardial strains based on the radial, circumferential, and longitudinal directions.

C. Myocardial Beads

Due to our image acquisition strategy [4], and our fitting approach that matches three sequences of orthogonal isoparametric planes to their corresponding tag planes, the intersection of three orthogonal isoparametric planes are the model's estimate of the 3-D position of tag plane intersections and are readily available for all time points at the conclusion of model fitting. We refer to these points as myocardial beads.

Viewing these intersection points in a cine-loop provides a good impression of the overall 4-D left ventricular motion. Fig. 2 shows a short-axis slice of a set of myocardial beads at end-diastole [Fig. 2(a)] and end-systole [Fig. 2(b)]. Also, Fig. 3 shows a long-axis view of several slices of myocardial beads at end-diastole [Fig. 3(a)] and end-systole [Fig. 3(b)]. Both sets of myocardial beads clearly show the deformation that occurs during the systolic phase of the cardiac cycle.

IV. RESULTS

We employed the tag detection method proposed in [3] to find the three sets of orthogonal tag lines for all image slices for all frames. Once tag lines in the short-axis and long-axis images are extracted and grouped by each tag plane for all frames of data, 4-D split Chamfer distance potentials are computed. The 4-D model then deforms in the potential fields within the constraints dictated by the model's internal energy. Finally, 3-D displacement and strain fields as well as myocardial beads are computed and visualized.

A. In Vivo Data

The method described was applied to tagged MR images collected from five normal human volunteers from end-diastole to end-systole. Once the tag lines were located in both the short-axis and long-axis slices for all frames, we used our 4-D B-spline model to calculate systolic myocardial strains. The computational time for fitting the model to image data from one study consisting of 10 frames of 10 short-axis and 13 long-axis images with a fourth-order (cubic spline) 4-D B-spline

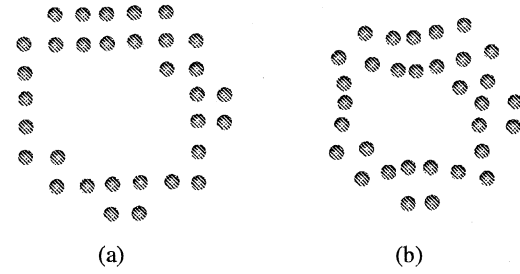


Fig. 2. Axial view of myocardial beads from a single basal slice at (a) end-diastole and (b) end-systole in a normal human volunteer.

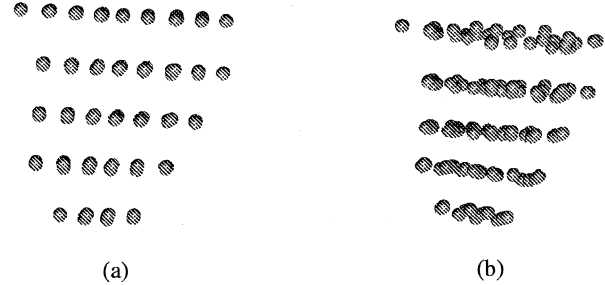


Fig. 3. Longitudinal view of myocardial beads from every other slice at (a) end-diastole and (b) end-systole in a normal human volunteer.

model of $17 \times 17 \times 12 \times 12$ control points was 295 min on a Sun Blade 100.

Since the method generates 3-D strain fields for all 3-D points over time, in order to reduce complexity of interpretation, we segment the entire LV wall into three layers: the base layer, the mid-ventricular layer, and the apical layer. Furthermore, the apical layer is segmented into four regions: anterior, lateral, inferior, and septal (A_{apex} , L_{apex} , I_{apex} , and S_{apex}), the mid-ventricular layer is segmented into six regions: antero-septal, anterior, lateral, posterior, inferior, and infero-septal (AS_{mid} , A_{mid} , L_{mid} , P_{mid} , I_{mid} , and IS_{mid}). Finally, the basal layer is segmented into antero-septal, anterior, lateral, posterior, inferior, and infero-septal (AS_{base} , A_{base} , L_{base} , P_{base} , I_{base} , and IS_{base}) regions. The average normal strains over each of the 16 segmented regions are plotted as a function of time. We then average across data sets by taking advantage of the temporal continuity of our model. One data set is selected to which all others are normalized based on the length of the systolic phase of the cardiac cycle. At each time point of our normalized data set, the strain values at the corresponding time point in every other data set is calculated. Average normal strains are shown in Fig. 4.

For all plots, end-diastole is assumed to occur at time $\tau = 0$ and is considered the reference undeformed state for calculating Lagrangian strains. The magnitude of strain values generally increases as the left ventricle contracts during systole. Since the plots only demonstrate strain values during systole, peak strain is typically achieved at the last time point shown.

B. Interpretation of Results

For normal strains, average radial, circumferential, and longitudinal strains are given in Fig. 4. The radial strains remain positive for most of the 16 regions indicative of the systolic thickening of the left ventricle. Both the circumferential and longitudinal strains are negative. Circumferential shortening during left ventricular contraction results in the negative strain values in the circumferential direction while compression in the longitudinal direction results in negative longitudinal strains. These results are comparable with other relevant work [2], [5].

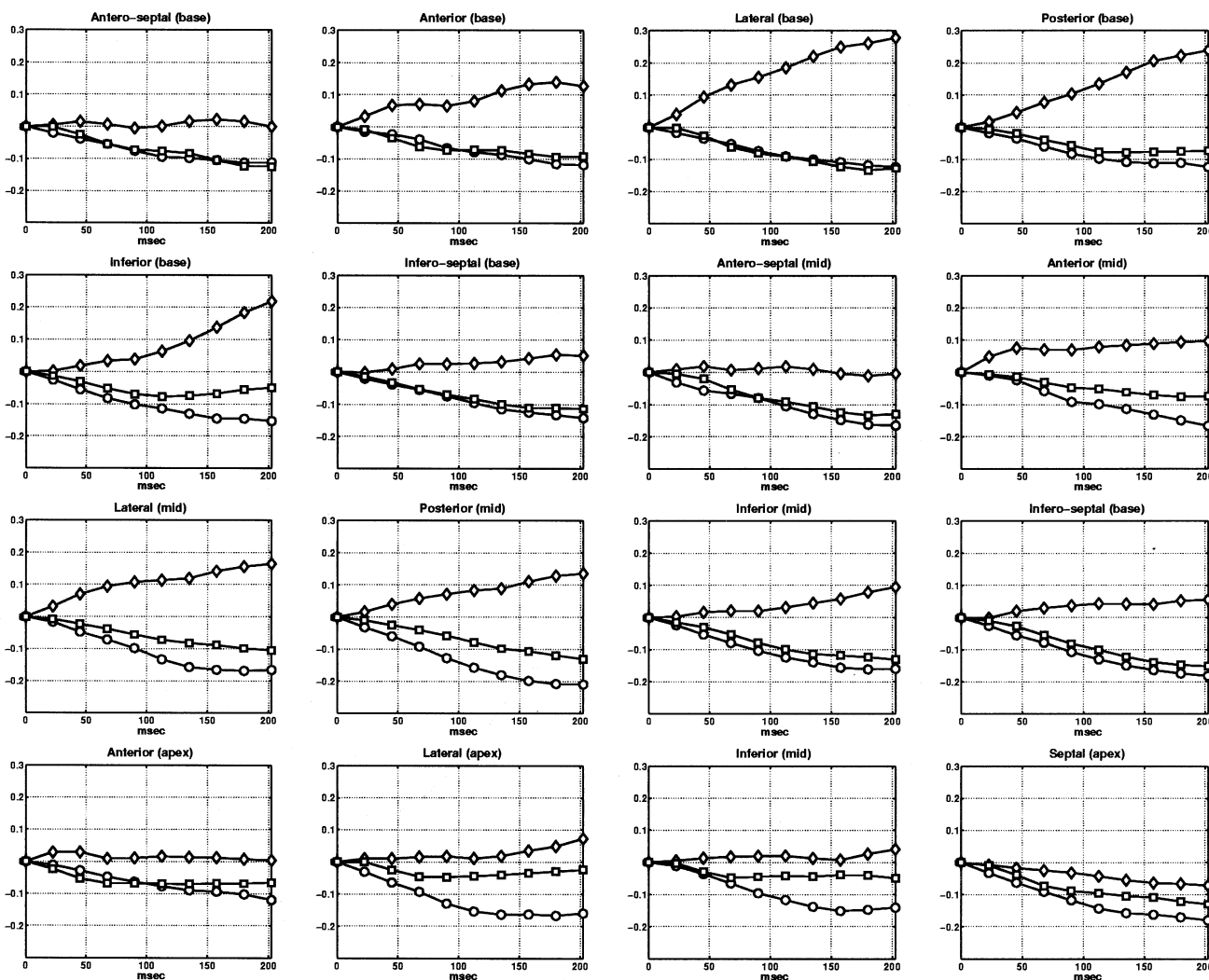


Fig. 4. Average normal strain plots across five normal human data sets for each of the 16 regions of the left ventricle. The different geometric shapes (diamond, circle, and square), represent the radial, circumferential, and longitudinal strain values, respectively. The x axis is the time in milliseconds during systole and the y axis is the strain value.

V. CONCLUSION

Our 4-D B-spline model is capable of producing comprehensive myocardial strain calculations for assessing myocardial viability by reconstructing 3-D displacement fields based on all available tag information. The novelty of the method is that at the conclusion of model fitting, 3-D myocardial displacements, 3-D myocardial strain maps, as well as 4-D locations of myocardial beads are immediately available. We illustrated these with results from five *in vivo* human studies. The resulting strain values were averaged across studies and plotted over the systolic phase of the cardiac cycle, and dynamics of cardiac deformations were visualized with a 3-D cine display of myocardial beads.

REFERENCES

- [1] E. A. Zerhouni, "Human heart: Tagging with MR imaging—A method for noninvasive assessment of myocardial motion," *Radiology*, vol. 169, pp. 59–63, 1988.
- [2] A. A. Amini and J. L. Prince, *Measurement of Cardiac Deformations from MRI: Physical and Mathematical Models*, A. A. Amini and J. L. Prince, Eds. Dordrecht, The Netherlands: Kluwer Academic, 2001.
- [3] Y. Chen and A. A. Amini, "A MAP framework for tag line detection in SPAMM data using Markov random fields on the B-spline solid," *IEEE Trans. Med. Imag.*, vol. 21, pp. 1110–1122, Sept. 2002.
- [4] J. Huang, D. Abendschein, V. G. Dávila-Román, and A. A. Amini, "Spatio-temporal tracking of myocardial deformations with a 4-D B-spline model," *IEEE Trans. Med. Imag.*, vol. 18, pp. 957–972, Oct. 1999.
- [5] C. C. Moore, C. H. Lugo-Olivieri, E. R. McVeigh, and E. A. Zerhouni, "Three-dimensional systolic strain patterns in the normal human left ventricle: Characterization with tagged MR imaging," *Radiology*, vol. 214, pp. 453–466, 2000.
- [6] J. Declerck, J. Feldmar, and N. Ayache, "Definition of a 4D continuous planispheric transformation for the tracking and the analysis of LV motion," *Med. Image Anal.*, vol. 4, no. 1, pp. 197–213, 1998.
- [7] C. Ozturk and E. R. McVeigh, "Four dimensional B-spline based motion analysis of tagged cardiac MR images," presented at the *SPIE Medical Image Analysis Conf.*, San Diego, CA, Feb. 1999.
- [8] W. S. Kerwin and J. L. Prince, "Cardiac material markers from tagged MR images," *Med. Image Anal.*, vol. 2, no. 4, pp. 339–353, 1998.
- [9] A. P. Borelli, *Elasticity in Engineering Mechanics*. Englewood Cliffs, NJ: Prentice-Hall, 1965.
- [10] W. H. Press, B. P. Flannery, S. A. Teukolsky, and W. T. Vetterling, *Numerical Recipes in C—The Art of Scientific Computing*. New York: Cambridge Univ. Press, 1988.